IAC–24–88849

Attitude determination of H-2A rocket bodies by using photometric measurements

Tomáš Hrobár[a*], Jiří Šilha[b], Peter Jevčák[c], Matej Zigo[d], Jakub Šilha[e], Palash Patole[f], Thomas Schildknecht[g]

[a] *Division of Astronomy and Astrophysics, Department of Astronomy, Physics of the Earth and Meteorology, Faculty of Mathematics, Physics and Informatics, Comenius University. Mlynska dolina, 842 48 Bratislava, Slovakia, tomas.hrobar@fmph.uniba.sk*
[b] *Division of Astronomy and Astrophysics, Department of Astronomy, Physics of the Earth and Meteorology, Faculty of Mathematics, Physics and Informatics, Comenius University. Mlynska dolina, 842 48 Bratislava, Slovakia,*
[c] *Division of Astronomy and Astrophysics, Department of Astronomy, Physics of the Earth and Meteorology, Faculty of Mathematics, Physics and Informatics, Comenius University. Mlynska dolina, 842 48 Bratislava, Slovakia,*
[d] *Astros Solutions s.r.o., Slovak Republic,*
[e] *Astros Solutions s.r.o., Slovak Republic,*
[f] *Astronomical Institute of the University of Bern, Switzerland,*
[g] *SwissSpace Association, Switzerland,*
[*] *Corresponding author*

Abstract

One of the most dangerous groups of debris objects for the long-term evolution of the debris population in Low-Earth Orbit (LEO) is the group of rocket bodies. They pose a significant threat and are one of the prime targets for active debris removal (ADR) missions due to their large size and orbital regimes. Precise estimation of rotational properties, such as rotation period and orientation of rotation axis, is essential for supporting potential ADR missions. For a specific type of rocket bodies, H-2A, one of the main candidates for removal, a special method was developed to determine the rotation axis orientation. This method is based on analysis of specular flashes. They occur when the phase angle bisector, vector dividing phase angle plane into two identical parts, is perpendicular to the object's highly reflective surface. in the case of H-2A the upper part is made of highly reflective material and causes specular flashes. These rocket bodies have cylindrical shape. It allows us to determine the rotation axis direction using the low-resolution Amplitude model. This model is ideal for cylindrical objects, assuming rotation around an axis perpendicular to the central axis in body-fixed reference frame. From the brightness ratio, which represents the difference between maximum and minimum brightness values during one rotation, the possible rotation axis orientation can be estimated. The brightness ratio depends on the object's position, tumbling axis orientation, and observer's location. Typically, when both the observer's location and object's position are known, we can derive the brightness ratio from the series photometric measurements. These methods require observations from different perspectives over a relatively short period, as large changes in the tumbling axis are not expected by the models. We present rotation axis estimations for H-2A rocket bodies, using two previously mentioned methods. H-2A rocket bodies are expected to rotate about an axis perpendicular to their central axis due to internal energy dissipation. Our results are based on photometric measurements from telescopes of private sector partners, AGO70 located in Slovakia and ZIMLAT located at the Swiss Optical Ground Station, Zimmerwald, Switzerland. Also archive data from Mini-Mega-Tortora (MMT) database and from the Space Debris Light Curve Database (SDLCD) are used.

Acronyms/Abbreviations

Space Debris Light Curve Database (SDLCD)

Mini-Mega-Tortora database (MMT)

70-centimeter Newtonian telescope located at the Astronomical and Geophysical Observatory in Modra (AGO70)

Low-Earth orbit (LEO)

Zimmerwald Laser and Astrometric Telescope (ZIMLAT)

Active debris removal (ADR)

In-orbit servicing (IOS)

1. Introduction

The space debris population consists of various types of objects with different shapes, material characteristics, and orbital parameters. These properties influence an object's attitude, rotation axis orientation, and rotational period. As the object orbits the Earth, it is subject to several natural forces that can significantly or slightly alter its attitude.

Determining the rotational properties of space debris is crucial not only for monitoring the population but also for assessing whether an object is suitable for ADR or if

its operational lifetime can be extended through IOS missions. For these missions, predicting the future evolution of rotational properties is essential. This evolution can be determined using simulators, with the current rotational properties serving as input.

The most used method for determining the orientation of the rotation axis, along with other parameters, involves simulating light curves. This process calculates the brightness of an object based on various parameters. The synthetic light curves generated from the simulations are then compared with observed light curves, and the one that most closely matches the observed data is considered to have the most accurate parameters. Some researchers only vary the coordinates of the rotation axis in their simulations, while others also adjust the object's dimensions [1]. Additionally, synthetic curves are generated using different material properties, sometimes even varying properties across different parts of the object [2]. These methods are computationally intensive and require large amounts of input data.

In this article, we present the results of the rotation axis orientation for objects belonging to the population of H-2A rocket bodies, using two methods. The first one is the low-resolution attitude determination method proposed by Williams [3] is well-suited for identifying the rotation axis orientation of cylindrical objects. The second, published by Vananti [4], is based on the time difference between specular flashes caused by the highly reflective surface of these rockets. Both methods are described in Sec. 3. The obtained results are presented in Sec. 4. These techniques require observing the target from multiple perspectives, or phase angles. However, this is not always possible from a single location due to weather conditions or the limited visibility of the object. Additionally, capturing faster changes in the rotation axis orientation demands higher time resolution in the photometric data and shorter intervals between data points, ensuring more accurate sampling of attitude variations.

The necessary photometric data on the brightness of objects were obtained from observations during a quasi-simultaneous campaign between the Faculty of Mathematics, Physics and Informatics, Comenius University in Bratislava, Slovakia, and the Astronomical Institute of the University of Bern, Switzerland. Additionally, archive data from the SDLCD and the MMT were used. The data sources are presented in Sec. 2.

2. Instrumentation and catalogues

The first instrument used in this study is the AGO70 (MPC code M34, 48.37N, 17.27E), operated by the Faculty of Mathematics, Physics, and Informatics at Comenius University in Bratislava. The telescope features a Newtonian design with an equatorial open fork mount (see Fig. 1). It is equipped with a CCD camera, the FLI-ProLine PL1001, which has an array size of 1024 x 1024 pixels, each measuring 24µm. The effective field of view is 28.5 x 28.5 arcminutes, with a pixel scale of 1.67 arcseconds per pixel. The primary mirror has a diameter of 0.7 meters and a focal length of 2962 mm. Recent upgrades allow the telescope to track LEO objects at altitudes higher than 700 km. The AGO70 is also fitted with Johnson-Cousins filters [5]. The data collected and processed are published in the SDLCD [6].

Fig. 1. AGO70 with its dome

The second system used is ZIMLAT, which has a one-meter aperture. Located at the Swiss Optical Ground Station and Geodynamics Observatory (MPC code 026, 46.88N, 7.47E) in Switzerland, it is operated by the Astronomical Institute of the University of Bern. This telescope employs a Ritchey-Chrétien design with an azimuth-elevation mount (see Fig. 2). It features a Nasmyth platform with four possible focal lengths: 1.2 m, 2 × 4 m, and 8 m, three of which are equipped with scientific instruments, including a Neo scientific CMOS tracking camera, a Spectral Instruments 1100 with a CCD sensor, and a single photon counter. The CCD camera sensor measures 30.7 mm x 31.0 mm, with a pixel size of 15 µm, and is equipped with a mechanical shutter. Mounted on a 4-meter focal length derotator platform, this setup provides a field of view of 13.2 x 13.3 arcminutes, with a pixel scale of 0.387 arcseconds per pixel. The telescope is shown inside its dome in Fig. 2.

Fig. 2. ZIMLAT with its dome (Photo credit: AIUB)

We used archive data from from the SDLCD [6], which includes over 1,900 light curves for 759 objects [7], maintained by the Faculty of Mathematics, Physics, and Informatics at Comenius University in Bratislava. Additionally, we will utilize data from the public MMT [8], which contains 400,000 light curves for 10,500 objects [7]. Both catalogues provide data for different objects, as well as overlapping objects.

3. Attitude determination for H-2A rocket bodies

3.1 Amplitude method

3.1.1 Method description

The Amplitude method is suitable only for cylindrical objects in stable end-over-end rotation (no precession and nutation). The most important relation is the Eq. 1, which expresses the apparent magnitude M of a cylindrical object that reflects light only by its sides and not its ends.

$$M = -2.5 \log_{10} \left(\frac{kla\gamma F}{R^2} \right) \qquad [1]$$

l in this relation is the length of the object, a is its radius, γ is albedo, F is a function of the phase angle and the orientation of the axis of rotation, R is the distance from the object to the observer and k is the solar constant.

The value F is given by Eq. 2 where $F1$ and $F2$ are defined by Eq. 4 and Eq. 5. The $function\frac{F_1}{F_2}$ is given by Eq. 3.

$$F = \frac{1}{4\pi} \left[\left(\pi - \text{function} \frac{F_1}{F_2} \right) F_2 + |F_1| \right] \qquad [2]$$

where $functionF_1/F_2$ is:

$$\text{function} \frac{F_1}{F_2} = \begin{cases} |\arctan \frac{F_1}{F_2}| & \text{if} \quad F_2 > 0 \\ \frac{\pi}{2} & \text{if} \quad F_2 = 0 \\ \pi - |\arctan \frac{F_1}{F_2}| & \text{if} \quad F_2 < 0 \end{cases} \qquad [3]$$

$$F_1 = \sin\phi \sin A_a |\sin \Gamma_a| \qquad [4]$$

$$F_2 = \cos^2 \frac{\phi}{2} - \sin^2 A_a . \left(\sin^2 \frac{\phi}{2} + \cos^2 \frac{\phi}{2} \cos^2 \Gamma_a \right) \qquad [5]$$

where A_a and Γ_a are polar angle and azimuth angle in model's coordinate system and ϕ is phase angle.

Because debris objects can rotate relatively fast (typically on the order of seconds up to hundreds of seconds [6]), the distance between the observer and the object does not change significantly during one rotation period. Then the change in brightness of the object during one rotation period is given by Eq. 6.

$$M_{max} - M_{min} = -2.5 \log_{10} \left(\frac{F_{max}}{F_{min}} \right) \qquad [6]$$

If the axis of rotation is perpendicular to the central axis, then the change in brightness during one period is given by only three parameters: the phase angle, and two coordinates of the rotation axis orientation. The difference between maximum and minimum brightness is called the brightness ratio. Thus, we can use this equation to calculate the orientation of the rotation axis if we know the brightness ratio and the phase angle of the object. It is clear that there are several pairs of coordinates that will lead to a similar value of the brightness values as measured, so it is necessary to have multiple measurements at different phase angles and look for those pairs that are the solution in all cases.

3.1.2 Method implementation

The attitude determination script is a Python script used to calculate the orientation of the rotation axis of cylindrical objects. The primary input parameters for this script are the observed brightness ratio, the associated error σ, and the geometric relationship between the observer, the object, and the Sun, derived from orbital elements valid for the observation dates [9].

The brightness ratio and its error are extracted using a light curve processing routine developed by the Faculty of Mathematics, Physics, and Informatics at Comenius University in Bratislava [6]. This routine is compatible with data from both the ZIMLAT and MMT.

The phase angle, as well as the vectors from the object to the Sun and from the object to the observer, are calculated using the positions of the observer, object, and Sun in the geocentric celestial reference system. The script computes the brightness ratio for every possible orientation of the rotation axis and generates a color map of these ratios. Next, it identifies the coordinates where the brightness ratio falls within ± σ of the observed value. These coordinates represent the potential directions of the tumbling axis for the specific phase angle.

The brightness ratio is calculated for each phase angle under which observations were made. If observations come from a single location, they must be taken at three different times. Once the brightness ratio is computed for all phase angles, the rotation axis orientations are transformed into the J2000 coordinate system. Finally, the script calculates and plots the intersection points of the possible rotation axis orientations for all observed phase angles, displayed in a 2D graph. These intersection points represent the most likely directions of the rotation axis.

3.2 Specular flashes method

3.2.1 Method description

This method was developed for specific part of space debris population. It is population H-2A rocket bodies. They all have similar shape (see Fig. Fig. 3. The method was published and used in [4] and is based on analysis of specular flashes. They occur when the phase angle bisector, vector dividing phase angle plane into two identical parts, is perpendicular to the object's highly reflective surface. In the case of H-2A the Payload support structure (PSS) is made of highly reflective material and causes specular flashes.

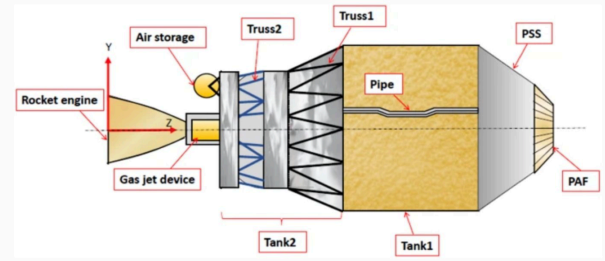

Fig. 3. H-2A upper stage [10]

The method presupposes that the object is in a flat spin state characterized by a consistent rotation axis h, with no precession, and unchanging angular momentum H. H and h are orthogonal to the axis of symmetry denoted as s. We define a coordinate system with axes x, y, and z, where z aligns with the phase angle bisector, and H lies in the $y-z$ plane. The origin of the coordinate system is the object's center of mass. In this setup, directions are associated with lines passing through the center of the sphere, and their representation involves their intersection points (projections) on the unit sphere (see Fig. 4). The orientation of the angular momentum H is expressed in spherical coordinates with an elevation angle δ_H and an azimuth angle $\alpha_H = 90°$. Specular reflection occurs when the bisector is perpendicular to an object's surface. The latitude line l_c represents possible directions of the cone axis satisfying specular reflection, tangent to the cone with

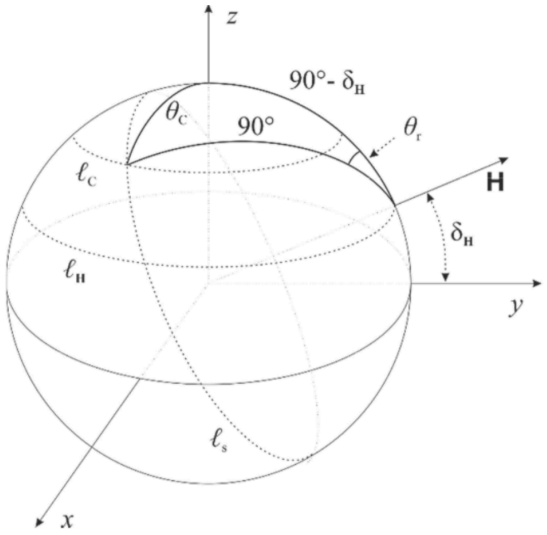

Fig. 4. Scheme showing the angular momentum direction H w.r.t. the phase angle bisector in z direction. The condition for specular reflection is given at the intersection of l_s (possible orientations of the body) and l_c (possible cone orientations for specular reflection). [4]

the plane perpendicular to the bisector z. The zenith angle at this latitude equals the cone aperture angle. The line l_s shows directions covered by s during the body's rotation around the axis h parallel to H. l_s lying in a plane perpendicular to H, forms a great circle on the sphere due to the object's flat spin. The intersection of l_s and l_c represents the orientation of s satisfying the specular reflection condition. The angle θ_r in the triangle is measured along the great circle l_s between the intersection point and the $y-z$ plane. An equivalent specular reflection condition can be identified at an angle $-\theta_r$ in the opposite position with respect to that plane. Referring to Fig. 4, the time interval between two close peaks is defined as t_p and the period of the light curve is marked T. If we define angular velocity ω, then $|\omega|T = 2\pi$ and $|\omega|t_p = 2\theta_r$ and we have definition of θ_r expressed in Eq. 7:

$$\theta_r = \frac{\pi t_p}{T} \qquad [7]$$

θ_r can be measured from lightcurve, θ_C is known from the shape of the rocket body and describes the angle between PSS and Tank 1 (Fig. 3). Then δ_H can be calculated by using spherical triangle and Eq. 8:

$$\delta_H = \pm \operatorname{acos}\left(\frac{\cos\theta_C}{\cos\theta_r}\right) \qquad [8]$$

Only δ_H can be determined by using this method. If we want to calculate also azimuth angle α_H we need to con-

vert the circle of δ_H to an inertial coordinate system and use another light curve to get another circle of possible solutions. Then the intersection of these two circles will be the orientation of the rotation axis of the object.

3.2.2 Method implementation

The script for determining the orientation of the rotation axis using the specular flashes method is implemented in Python. The input data consists of the time interval between the two nearest specular flashes, the rotational period of the object, the object's orbital elements, as well as the time and location of the observations. The time interval between the two closest specular flashes is extracted from the light curve by calculating the time difference between the occurrences of the flashes. Based on this data, the position and the phase angle bisector are determined. Subsequently, δ_H is computed through an established equation, and vectors forming an angle of 90° - δ_H with the phase angle bisector are identified. These vectors are then transformed into right ascension and declination in the J2000 reference frame. This procedure is performed for all observational data, and the intersection of the solutions from each observation is determined to identify the most probable orientation of the rotation axis.

4. Results

In this section, we present the results of the rotation axis calculations for two objects. One was observed during a campaign conducted in 2023, involving AGO70 and ZIMLAT. For the results of the second object, archival data from the SDLCD and MMT catalogues were used. For the application of the Amplitude Method, specular flashes were removed from the light curves, and 10 percent of the brightness ratio value was used as sigma. For the specular flash method, the time of the flash's maximum ±0.5 second was selected as the moment when the specular flash occurred. Typical lightcurve of H-2A is shown in Fig. 5.Specular flashes can be seen as significant peaks.

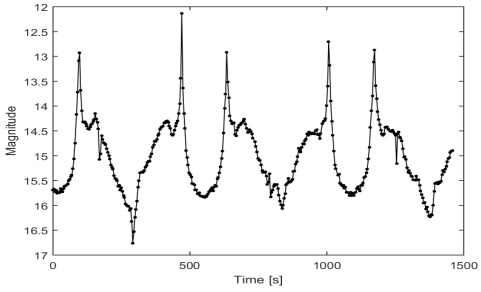

Fig. 5. Lightcurve of 28938, 2006-004B observed with AGO70

4.1 NORAD 37159, COSPAR 2010-045B

The object is no longer on orbit. We used archival data from the MMT and SDLCD catalogs covering the period from September 21 to September 23, 2020. We were able to gather enough data to calculate the rotation axis orientation at intervals of just 50 hours apart (see Table 1). Using two methods, we obtained a total of four solutions (along with their respective opposite directions, as these methods are unable to distinguish the sense of rotation, see Table 2), two of which are nearly identical. The approximate coordinates of this solution are: RA= 219° and DEC= 31° (see Fig. 6).

Table 1. Acquired observation data for 37159, 2010-045B from two different catalogues

Source	Series Start (UTC)	Distanstance [km]
MMT	21:31, September 21, 2020	11 764
SDLCD	23:27, September 22, 2020	16 630
MMT	00:02, September 23, 2020	16 791

Table 2. Results for rotation axis orientation of 37159, 2010-045B

Method	Right ascension [degrees]	Declination [degrees]
Amplitude	219	30
Amplitude	173	-60
Specular flashes	158	-60
Specular flashes	219	33

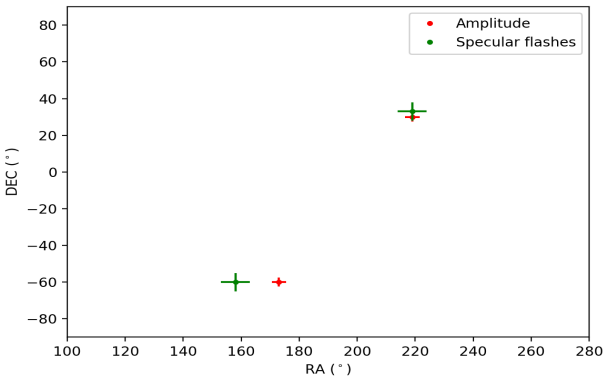

Fig. 6. Results for rotation axis orientation of 37159, 2010-045B using Amplitude method (red) and Specular flashes method (green)

4.2 NORAD 26899, COSPAR 2001-038B

The object is in an orbit with a perigee altitude of approximately 250 km and an apogee altitude of around 31,000 km. We used observation data acquired during one night (see Table 3). This is important for objects in similar orbits, as they are regularly exposed to atmospheric drag and gravitational torque, which can alter their attitude. Both methods produced two potential solutions (along with their respective opposite directions, see Table 4).Two solution regions are in close proximity to each other, approximately RA= 61° and DEC= -42° (see Fig.7).

Table 3. Acquired observation data for NORAD 26899, COSPAR 2001-038B from two different sensors

Sensor	Series Start (UTC)	Distanstance [km]
AGO70	21:57, May 31, 2023	34 412
AGO70	23:32, May 31, 2023	32 025
ZIMLAT	01:51, June 1, 2023	16 962

Table 4. Results for rotation axis orientation of 26899, 2001-038B

Method	Right ascension [degrees]	Declination [degrees]
Amplitude	103	55
Amplitude	65	-39
Specular flashes	56	-44
Specular flashes	62	58

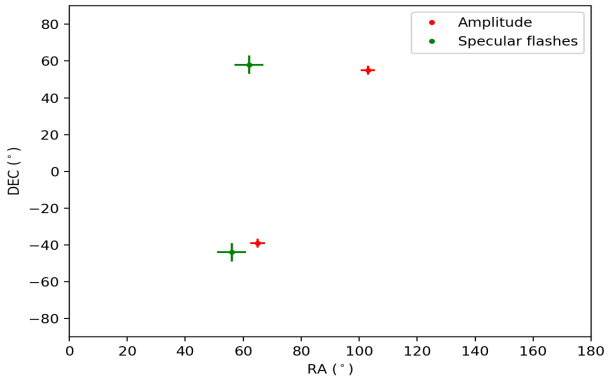

Fig. 7. Results for rotation axis orientation of 26899, 2001-038B using Amplitude method (red) and Specular flashes method (green)

5. Discussion

In this paper, we presented the results of calculating the rotational axis orientation for two H-2A rocket bodies. Two methods were used for this calculation: the Amplitude Method [3] and the Specular Flashes Method [4]. To apply these methods, the object must be observed at various phase angles, but within a short enough time frame to ensure that the rotational axis orientation remains unchanged. For this purpose, we used data from two catalogs and two sensors. In both cases, we found one solution region that was common to the results of both methods. We demonstrated that the methods can also be applied to quasi-simultaneous observations from different locations, as collecting sufficient data from a single site can be challenging.

While searching for suitable candidates for applying the two mentioned methods, we also found objects where the time interval between two specular flashes was greater than allowed by the Eq. 8. This could indicate that the object is not in simple rotation and rotation axis has precession. This will be the subject of further research.

The largest source of error was the precise determination of the time at which the specular flash occurred. To refine this, we will use the sensor network of Astros Solutions s.r.o., which is capable of observing objects at a high cadence (see Fig. 8) and thus improving the accuracy of specular flash timing.

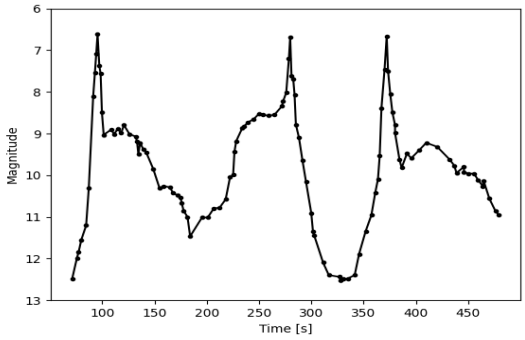

Fig. 8. Lightcurve of 28938, 2006-004B observed by Astros Solutions s.r.o

References

[1] T. Yanagisawa and H. Kurosaki, "Shape and motion estimate of leo debris using light curves," *Advances in Space Research*, vol. 50, no. 1, pp. 136–145, 2012.

[2] L. D. Blacketer, H. G. Lewis, and H. Urrutxua, "A technique for rotation vector position determination for tumbling rocket bodies," in *First International Orbital Debris Conference*, 2019.

[3] V. Williams, "Location of the rotation axis of a tumbling cylindrical earth satellite by using visual observations: Part i: Theory," *Planetary and Space Science*, vol. 27, no. 6, pp. 885–890, 1979.

[4] A. Vananti, Y. Lu, and T. Schildknecht, "Attitude estimation of h2a rocket body from light curve measurements," *International Journal of Astrophysics and Space Science*, vol. 11, no. 2, pp. 15–22, 2023.

[5] M. Zigo, J. Šilha, T. Hrobár, and P. Jevčák, "Space debris surface characterization through bvrcic photometry," *Advances in Space Research*, vol. 72, no. 9, pp. 3802–3817, 2023.

[6] J. Šilha *et al.*, "Space debris observations with the slovak ago70 telescope: Astrometry and light curves," *Advances in Space Research*, vol. 65, no. 8, pp. 2018–2035, 2020.

[7] J. Šilha, P. Jevcák, M. Zigo, T. Hrobár, and A. Szilágyi-Sándor, "Photometric phase functions of resident space objects and space debris extracted from brightness measurements," in *Proceedings of the Advanced Maui Optical and Space Surveillance (AMOS) Technologies Conference*, 2023, p. 178.

[8] S. Karpov *et al.*, "Mini-mega-tortora wide-field monitoring system with sub-second temporal resolution: First year of operation," *Revista Mexicana de Astronomía y Astrofísica*, vol. 48, pp. 91–96, 2016.

[9] USSTRATCOM, *SpaceTrack*, `https://www.space-track.org/documentation/faq`, Online; Accessed: 13.09.2024, 2023.

[10] T. Yanagisawa, M. Hayashi, H. Kurosaki, and S. Kawamoto, "Correlation between light curve observations and laboratory experiments using a debris scale model in an optical simulator," *Advances in Astronautics Science and Technology*, vol. 4, no. 1, pp. 47–54, 2021.